

## EFFECT OF UNPROTECTED INTERIOR BEAMS ON Membrane Behaviour of Composite Floor Systems in Fire. II: Numerical Assessment

Tuan-Trung Nguyen <sup>a</sup>, Kang-Hai Tan <sup>a</sup>

<sup>a</sup> Nanyang Technological University, School of Civil and Environmental Engineering, Singapore

### Abstract

The authors' companion paper presented the observations and results from two one-fourth scale composite beam-slab systems tested in fire. This paper introduces the numerical assessment based on these experimental results. A non-linear finite element model is developed using ABAQUS/Explicit to simulate the specimen behaviour. Material properties at elevated temperatures are assumed to vary according to EN 1994-1-2 (2005). The FE model was first validated with the test results, and then was used to examine the effect of unprotected interior beams on tensile membrane action. It is found that the numerical predictions agree well with the test results. The presence of interior beams significantly affects the magnitude as well as the distribution of stress of the slab elements, i.e. mesh reinforcement and concrete slab. The part with maximum tensile force is not necessarily at the slab centre. It may be part of the concrete slab above the edge beams. Shortcomings of the numerical model in predicting the failure modes are indicated.

**Keywords:** finite element analysis, composite floor systems, tensile membrane action, fire

### INTRODUCTION

This paper describes numerical assessments of the effect of unprotected interior beams on the membrane behaviour of composite beam-slab systems in fire. A nonlinear finite-element model is developed using ABAQUS/Explicit and validated against the experimental results presented in the companion paper in terms of temperature development, deflection response, and failure modes. The validated model provides valuable insight into the stress and strain distribution of concrete and reinforcement at the membrane stage of the systems.

This paper uses the experimental results from two tested specimens which are denoted as S2-FR-IB and S3-FR. S3-FR was designed without any interior beam, while S2-FR-IB had two interior beams. The layout of the two specimens is shown in Fig. 1, in which the notation MB, PSB, and USB denote protected main beam, protected secondary beam, and unprotected secondary (interior) beam, respectively.

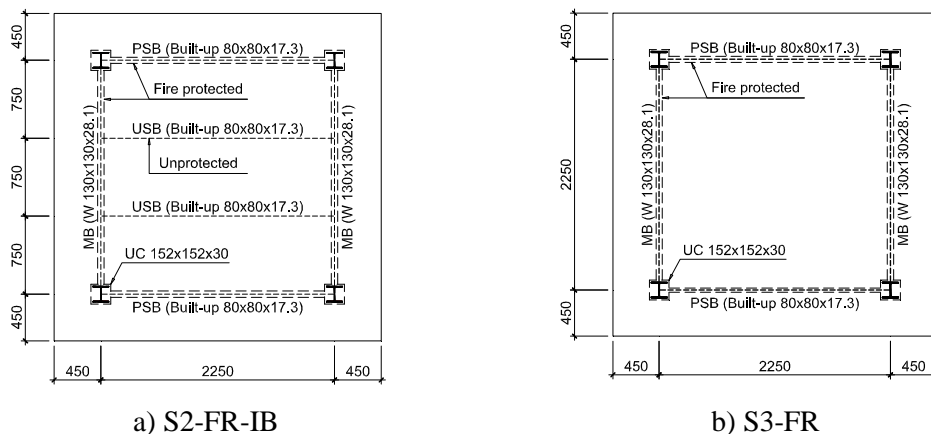


Fig. 1 Structural layout of the specimens

Both slabs are considered as rotationally restrained by the additional beam system placed on top of the outstand part. The beam system was fixed to the reaction frame. More details can be found in the authors' companion paper.

## 1 MODELLING TECHNIQUE

ABAQUS/Explicit was adopted because it uses consistent large-deformation theory which can overcome the numerical convergence difficulty caused by the simulation of large-deformation problems. *Sequentially coupled thermal-stress analysis procedure* is used because the thermal fields are the driving forces for the stress analysis but the thermal solution does not depend on the stress solution. Therefore, the simulation comprises two steps: (1) apply mechanical loading; (2) apply heating. *Concrete damaged plasticity model* was adopted, and reinforcement was modelled using the layered rebar technique.

S4R shell element was used to discretize both the beams and the slabs. Fully composite action between the beams and the slab was simulated using 'tied' technique via surface-based contact interactions.

Material properties of the steel and the concrete were obtained from tensile coupon tests and concrete cylinder tests at ambient temperature. The corresponding material properties at elevated temperatures were then obtained using the material reduction factors specified in EN 1994-1-2 (2005). For numerical purposes, the descending branches of concrete and reinforcement models were also adopted. Therefore ultimate compressive strain of concrete was taken from Table B.1 EN 1994-1-2, which depends on temperature of concrete slab; and ultimate tensile strain of reinforcement was taken as 0.2.

The simplified numerical model took into account the steel beams, the concrete slab, and the reinforcing mesh. Vertical support for the slab edges was provided by the protected edge beams. In turn, these beams were supported by the columns. Vertical restraint ( $U_3 = 0$ ) was imposed at the column locations; it is assumed that the vertical displacement at these positions is negligible. Vertical restraint along the edge outstands was applied to model the rotational restraint beam system, which was assumed to provide infinite vertical stiffness.

The temperature distribution at the slab bottom surface was incorporated into the numerical model. Based on the recorded temperatures at the mesh reinforcement and at the slab top surface, thermal gradient across the slab thickness was defined. For the beams, the recorded temperatures across the beam sections were incorporated into the model.

## 2 MODEL VALIDATION

### 2.1 Temperature Development

Figs. 2 and 3 show the comparisons of the temperature distribution of the slabs between the simulation and the test results. With a thermal gradient of  $10^\circ\text{C}/\text{mm}$ , the predicted temperatures agreed very well with the experimental results.

However, the results were not very good for the mesh temperature in S3-FR after 22min of heating. This is because severe cracks appeared in S3-FR resulting in significant heat losses. Consequently, the recorded mesh temperature increased at a lower rate after the cracks had appeared.

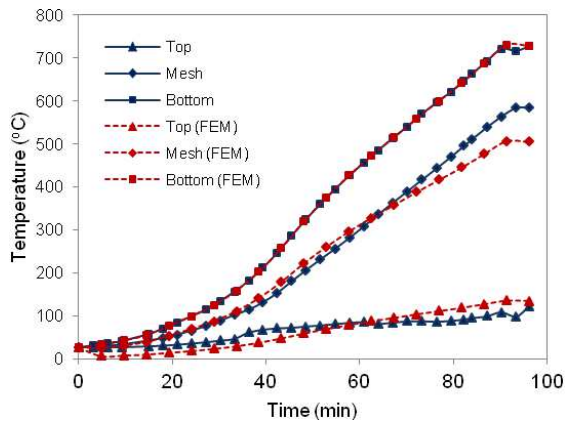


Fig. 2 Temperature distribution – S2-FR-IB

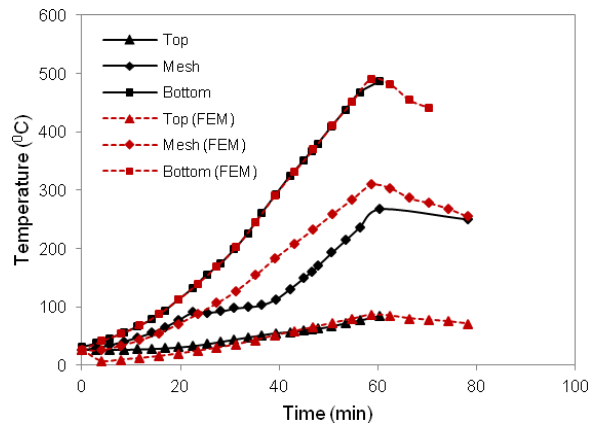


Fig. 3 Temperature distribution – S3-FR

## 2.2 Slab / Beam Deflection

Recorded temperature profiles of the flanges and the webs of the beams were input directly into the numerical models using the amplitude technique in ABAQUS. Consequently, structural behaviour can be obtained. Comparisons in terms of beam deflections versus time, as shown in Figs. 4 and 5, demonstrate that the model predicts the beam and the slab behaviour very well.

However, for the main beam of S3-FR the comparison is poor although the trend is similar. This is because in S3-FR severe cracks appeared at a very early stage (just 20min into the start of heating), directly above the main beams. Thus, composite action between the main beams and the slab could not be maintained, leading to inaccurate measurements of the beam deflection. These measurements were taken from the part of the concrete slab directly above the beams.

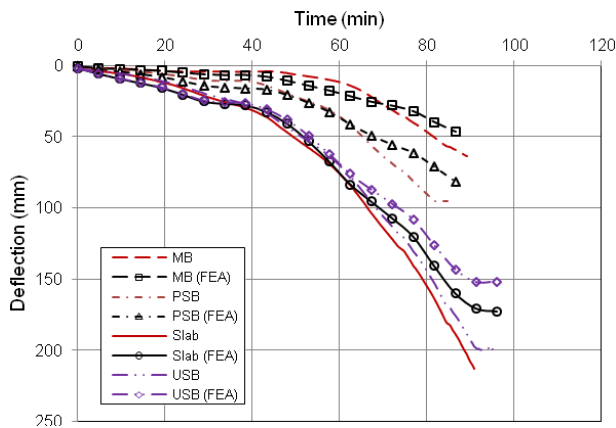


Fig. 4 Deflection vs. time curves for S2-FR-IB

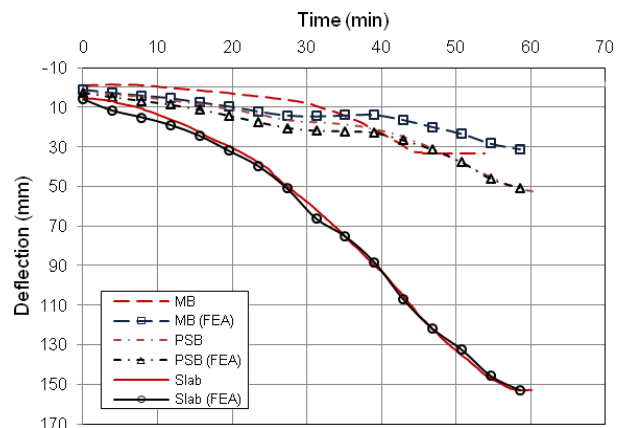


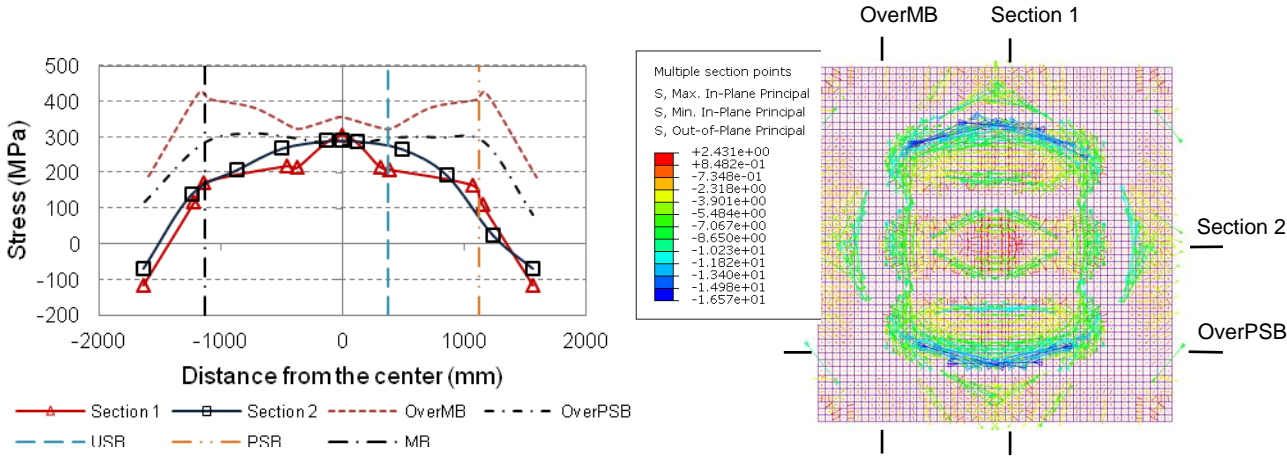
Fig. 5 Deflection vs. time curves for S3-FR

Fig. 4 also shows the deflection of unprotected interior beam of S2-FR-IB. As expected, the mid-span deflection of the beam was very close to that of the slab even though the beam was not at the slab centre. This indicates that the slab behaved as a membrane. This membrane was supported by the reinforcement mesh which anchored into the protected edge beams.

## 3 DISCUSSION

Figs. 6 and 7 show the stress distributions across the sections and at the top surface of the slabs at failure. In these figures, Section 1 denotes the mid-span slab section perpendicular to

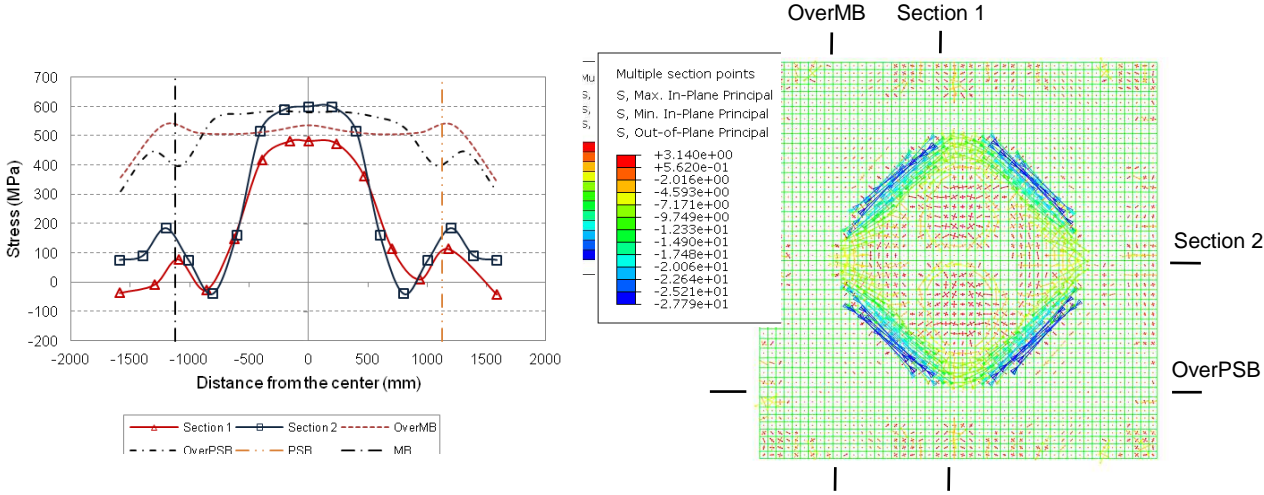
the protected secondary beams, Section 2 denotes the mid-span slab section perpendicular to the main beams, OverMB is the cross slab section above a main beam, and OverPSB is the cross slab section above a protected secondary beam. The positions of these cross sections are indicated in Figs. 6(b) and 7(b).



a) Stress distributions in reinforcement cross sections      b) Stress distribution at concrete top surface

Fig. 6 Stress distribution of S2-FR-IB at failure – 84.0min

It can be seen that, for S2-FR-IB, at 84.0min the maximum tensile stress of 425MPa in the reinforcement is found above the main beam. The maximum stress above the protected secondary beams is 310MPa, approximately equal to the stress in the reinforcement across the slab mid-span section. For S3-FR, the maximum tensile stress is found at the slab mid-span (Section2), followed by the section above the protected secondary beam (OverPSB).



a) Stress distributions in reinforcement cross sections      b) Stress distribution at concrete top surface

Fig. 7 Stress distribution of S3-FR at failure – 45.0min

The principal stress distributions at the top surface of the concrete slab are shown in Figs. 6(b) and 7(b), in which negative values indicate compressive stresses and positive values indicate tensile stresses. It can be seen that TMA was obviously mobilized in all specimens, with the formation of a tensile zone in the slab centre and a ‘compression ring’ consisting of the upper parts of the edge beams and part of the concrete slab directly above the edge beams.

The compression ring was most evident in S2-FR-IB, but it was not so clearly observed in S3-FR. This is possibly because the tensile stresses in the central zone of the slab in S3-FR were mainly equilibrated by the compressive stresses in the upper parts of the steel edge beams, with some contribution from the compressive stresses in the concrete slab. It should be noted that S3-FR was designed without any interior beam. Therefore tensile stress at the slab centre region in S3-FR is quite uniform and continuous, which is not observed in S2-FR-IB. In S2-FR-IB, part of concrete slab above the unprotected interior beams is still in compressive because of the effect of T-flange beam.

Therefore, on the basis of numerical simulations of S2-FR-IB (Fig. 6), the fracture of reinforcement above the edge beams would occur first, before the fracture of the reinforcement at the mid-span of the slabs; this failure mode concurs with the experimental observations.

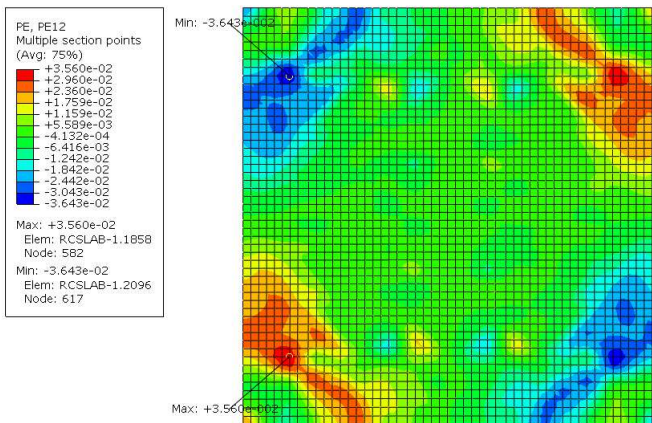


Fig. 8 Strain distribution at top surface – S2-FR-IB at failure – 84.0min

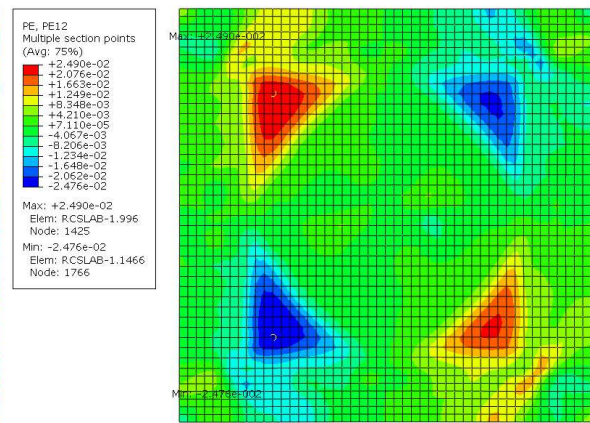


Fig. 9 Strain distribution at top surface – S3-FR at failure – 45.0min

In S3-FR, failure is predicted to be due to fracture of reinforcement at the slab mid-span. However, in the actual test, the failure mode was due to the failure of compression ring. On the other hand, as shown in Figs. 8 and 9, the maximum strain at the top surface of the concrete slab at its corners is 0.0356 and 0.0249 for S2-FR-IB and S3-FR, respectively. These values are higher than the failure compressive strain according to EN 1994-1-2, which are 0.0223 for S2-FR-IB and 0.0213 for S3-FR at the same temperature of the concrete slab. It means that at the slab corners, the stress in concrete top surface is almost zero, or failure would occur in these regions. Unfortunately, there is no obvious indication of which failure mode, i.e. reinforcement fracture at the slab mid-span or concrete crushing at the slab corner, would occur first. This is a shortcoming of the numerical model.

Although the comparisons show good correlation between test and numerical results for both specimens, there are still several limitations of the numerical model. Firstly, final failure modes of the beam-slab substructures could not be exactly identified from the stress or strain contours. Secondly, partial failures such as concrete crushing and fractures of rebars can not be taken into account. Also, heat loss caused by the appearance of concrete cracks could not be predicted.

#### 4 CONCLUSION

This paper presents numerical studies on the effect of interior beams on membrane behaviour of composite slab-beam systems in fire. The proposed numerical model was validated with the test results of two specimens, and the results show good correlation between the test and the numerical results.

It is found that the presence of interior beams significantly affects the magnitude as well as the distribution of stresses in the slab elements. The maximum tensile stress is not necessarily

located at the slab centre, but may be located in the concrete slab above the edge beams. This may cause different failure modes for the floor assemblies compared with those of isolated slab panels.

## **5 ACKNOWLEDGEMENT**

The authors would like to acknowledge the support provided by Agency for Science, Technology and Research (A\*Star Singapore) for this work under Grant No. 0921420047.

## **REFERENCES**

- Abu, A. K., I. W. Burgess, et al., Slab panel vertical support and tensile membrane action in fire. *Steel and Composite Structures* 8 3 (2008), 217-230, 2008.
- EN 1994-1-2: *Eurocode 4. Design of composite steel and concrete structures - Part 1-2: General Rules - Structural fire design*. Brussels, Belgium, European Committee for Standardization (CEN), 2005.